Strål
säkerhets
myndigheten

Swedish Radiation Safety Authority

Authors: V. Dykin
A. Hernández-Solis
C. Demazière

Research

2014:09

Further Development of the Core Simulator CORE SIM: Extension to coupled capabilities for BWRs

Report number: 2014:09 ISSN: 2000-0456
Available at www.stralsakerhetsmyndigheten.se

SSM perspective

Background

Noise analysis and diagnostics is of prime importance for an early detection of anomalies, as well as for determining some parameters of the system. As a consequence, the use of noise analysis/diagnostics contributes to improved nuclear reactor safety.

In 2004, the neutronic tool called CORE SIM was developed and finalized to model the fluctuations in neutron flux in PWRs/BWRs. This first model was based on solving two-group diffusion equations in 2 dimensions. Later on, in 2011, CORE SIM was modified in order to be able to handle three dimensional systems.

Objectives of the project

The aim of the present research project is to extend the CORE SIM tool with a two phase thermo-hydraulic model in such a way that it can also model fluctuations in BWRs in a more realistic manner. Such a complemented tool will provide an opportunity to study different phenomena which took place in the past in BWRs such as, for example, density wave oscillations.

Results

The developed tool is fully MatLab based and requires a set of input data from a commercial static core simulator. The driving perturbation can be specified both as a perturbation in thermo-hydraulic parameters or directly as a perturbation in macroscopic cross-sections. As output, the 3-dimensional spatial distribution of the noise in coolant density, pressure, enthalpy, inlet velocity, fuel temperature and neutron flux is obtained.

In this work, some results of the noise simulations, performed for the case of a homogeneous perturbation in inlet velocity for a commercial reactor core are shown and discussed. All calculations are performed in 3D node-wise space and frequency domain.

Applications

The extended CORE SIM core simulator, now being able to treat for PWR and BWR systems, can be used especially for studying different phenomena taking place in commercial power plants such as, for example, the effect of density wave oscillations and related local instabilities in BWRs. Another application of this tool is that it could be used to identify the origin of the increasing low-frequency noise level, recently observed in Swedish and German PWRs.

Project information

Responsible at SSM has been Ninos Garis.
SSM references: SSM 2012/3299

Strål
säkerhets
myndigheten

Swedish Radiation Safety Authority

Authors: V. Dykin, A. Hernández-Solis and C. Demazière
Chalmers University of Technology, Department of Nuclear Engineering

2014:09

Further Development of the Core Simulator CORE SIM: Extension to coupled capabilities for BWRs

Date: November 2013
Report number: 2014:09 ISSN: 2000-0456
Available at www.stralsakerhetsmyndigheten.se

Sammanfattning

Även om en kärnreaktor körs i konstant drift, finns en viss inneboende fluktuation av processparametrarna. Dessa fluktuationer kan användas för att diagnosticera avvikelser eller för att verifiera dynamiken i reaktorn. Det är därför av stor säkerhetsmässig betydelse att kunna mäta fluktuationer kontinuerligt. Vanligtvis kräver tolkningen av fluktuationsmätningar att man känner reaktorns överföringsfunktion, vilken innehåller systemets respons på en pålagd fluktuation. I denna rapport presenteras arbete utfört vid avdelningen för nukleär teknik, institutionen för teknisk fysik, Chalmers tekniska högskola. Syftet med arbetet är att utveckla modellverktygen som behövs för att bestämma överföringsfunktionen. På grund av den starka kopplingen mellan neutrontransport och värmetransport i kylmediet används multifysikmodeller. Arbetet ingår i en långsiktig och pågående satsning för att förbättra modelleringsverktygen för lättvattenreaktorer. En numerisk metodik har utvecklats och testats för tryckvattenreaktorer, vilket är den globalt vanligaste reaktortypen men som i Sverige endast finns i Ringhals. I denna rapport sammanfattas vidareutvecklingen och testerna av denna numeriska metodik för att utvidga den till kokvattenreaktorer, vilket innebär att metodiken blir tillämplig för samtliga svenska reaktorer.

Extended abstract

In nuclear reactors, the monitoring of the nuclear core is of prime importance for guaranteeing the safety of the plant. Assuming stationary conditions, the measurement of process signals using the existing instrumentation supplemented by adequate data acquisition chains allows monitoring fluctuations of the process signals around their mean values. Even though the system does not exhibit any change in the mean values of the process signals, these fluctuations are always present and are the result of e.g. the turbulent character of the cooling flow, coolant evaporation, and/or possible anomalies (excessive vibrations, etc.). These fluctuations (often referred to as “noise”) thus carry some information about the dynamics of the system, and can be used either for core diagnostics/surveillance purposes (i.e. when an anomaly is suspected in the core) or for determining dynamical core parameters/safety coefficients. The main advantage of such techniques relies on the fact that no perturbation of the system is required and that the method is thus a non-intrusive one.

The instrumentation present in nuclear core mostly consists of neutron detectors. Many neutron noise diagnostics tasks thus involve an inversion or „unfolding“ procedure, where the neutron noise measured in a few locations throughout the nuclear core is used to determine the root cause (i.e. noise source) responsible for the measured neutron noise. Such an inversion is seldom possible without the knowledge of the so-called reactor transfer function, i.e. the function giving the neutron noise induced by any arbitrary noise source. The Division of Nuclear Engineering at Chalmers University of Technology has been very active for the last ten years in developing computational methods allowing the estimation of such a transfer function for actual reactor cores, i.e. strongly non-homogeneous systems.

A numerical tool, named CORE SIM, was developed to estimate the open-loop reactor transfer function. In this tool, the noise source is defined in terms of fluctuations of the macroscopic cross-sections. This report deals with the development of a thermal-hydraulic module coupled to CORE SIM, so that the closed-loop reactor transfer function can also be estimated for Boiling Water Reactors (which is the main type of reactors constituting the Swedish fleet). This module is based on solving the mass, momentum, and enthalpy conservation equations for the fluid, and on solving the heat conduction equation in the solid fuel pellets. Because of the fully coupled neutronic/thermal-hydraulic character of the tool, the noise source can be directly defined in more realistic terms such as perturbations of the flow velocity, temperature, etc. at the inlet of the core. The coupled tool, in addition to be the only one of its kind, has a wide range of applicability.

Contents

1 Introduction

The proper diagnostics and monitoring of the properties of a reactor core and its internals is one of the main issues in detecting and determining core anomalies at early stages. Today, there exist several methods of core diagnostics; however most of them rely on the disruption of a reactor operation. An alternative way is to use so-called noise-based methods where small fluctuations of the neutron flux around its mean value are studied both in space and time (or frequency). The main advantage of this method is that it does not require any disturbance of a reactor system and can be used for on-line monitoring of the reactor properties. The neutron noise diagnostics methods have already been widely used in the past to determine reactor safety parameters such as Moderator Temperature Coefficient (MTC), coolant velocity etc. (Demazière C. et. al., 2008, 2009).

Noise analysis and diagnostics is of prime importance for an early detection of anomalies, as well as for determining some parameters of the system. As a consequence, the use of noise analysis/diagnostics contributes to improved nuclear reactor safety.

The main goal of neutron noise diagnostics is to elaborate different techniques which can help to “unfold” neutron noise sources, i.e. the perturbations which drive the fluctuations in the neutron flux, from the corresponding neutron flux measurements. However, the successful unfolding of a neutron noise source, usually requires the knowledge about the reactor transfer function as well as an access to full spatial distribution of the neutron noise. Unfortunately, in real power plant systems, the measuring capabilities are limited with just a few detectors and, as a result, the neutron flux can not be measured in each point of interest. The latter means that the full spatial reconstruction of the neutron fluctuations over an entire reactor core with an application of the existing power plant equipment is simply not possible. Such a problem can partially be resolved if one has a possibility to numerically estimate the neutron noise due to different types of perturbations. Comparing these results of a numerical prediction with the corresponding neutron flux measurements, the conclusion about the type of original perturbation can be drawn.

Several efforts in developing special tools for such a numerical estimation of the neutron noise have already been undertaken at the Division of Nuclear Engineering, Department of Applied Physics, Chalmers University of Technology. Thus, in 2004, the neutronic tool called CORE SIM was developed and finalized to model the fluctuations in neutron flux in PWRs/BWRs. This first model was based on solving two-group diffusion equations in 2 dimensions via so-called Greens function technique (Demazière C. et. al., 2004). Later on, in 2011, CORE SIM was modified in order to be able to handle three dimensional systems (Demazière C. et. al., 2011). Despite good qualitative results obtained from these two models, both of them represented open-loop systems i.e. they did not account for any thermo-hydraulic feedbacks. The latter fact led to a somewhat artificial way of introducing a perturbation in these models where the neutron noise source was specified as a perturbation in the relative macroscopic cross-section(s). In real reactor systems, the fluctuations in the neutron flux are usually caused by various thermo-hydraulic fluctuations which are then transferred into the fluctuations of macroscopic cross-sections. In order to take into account such a physical coupling, it was suggested to compliment the existing CORE SIM tool with a simple single-phase thermo-hydraulic model. Such an extension of the CORE SIM tool was performed as a PhD project in 2012 (Larsson V. et. al., 2012) and resulted in a sophisticated numerical tool which is capable to simulate realistic fluctuations in PWRs. This newly-developed tool was also benchmarked against other existing commercial tools such as RELAP-PARCS where a satisfactory qualitative agreement between the two models was obtained.

Since the introduced thermo-hydraulic model was a single-phase one, the application of the CORE SIM tool was only limited to PWRs. The aim of the present research project is to extend the CORE SIM tool with a two phase thermo-hydraulic model in such a way that it can also model fluctuations in BWRs in a more realistic manner. It is clear that the simultaneous presence of two phases in the coolant density makes the system quite heterogeneous. As a result, the extension of CORE SIM with the thermo-hydraulic model becomes an even more important issue for BWRs than for PWRs. In addition, such a complemented tool will also provide an opportunity to study different phenomena which took place in the past in BWRs such as, for example, density wave oscillations.

The work performed during this project is summarized below.

First, as is customary in reactor noise theory, the corresponding static solution of the system should be found. For this reason, the main features of a steady–state calculation model, including both a neutronic module based on the earlier-developed CORE SIM core simulator and a newly-developed two-phase thermo-hydraulic module together with the respective coupling procedures are presented.

Further, the iterative schemes used to perform steady-state calculations, are pointed out. Some results of static calculations showing the axial distributions of the thermal neutron flux and coolant density are following up.

Next, the description of the models utilized in noise calculations, both the neutronic and thermo-hydraulic ones as well as their coupling is given. Similarly to the static case, numerical methods implemented in the dynamical calculations are also touched upon.

Finally, as an illustration of the capabilities of the tool, some results of the noise simulations, performed for the case of a homogeneous perturbation in inlet velocity for a commercial reactor core are shown and discussed. All calculations are performed in 3D node-wise space and frequency domain.

2 Static calculations

2.1 Derivation of the static equations

In this section, the time-independent governing equations that describe the interaction among the different neutronic and thermal-hydraulic variables in the core are described. The aim is to solve a coupled model as a function of space, where the nodal thermal-hydraulic feedback that exists in a BWR is properly taken into account by the nodal neutron flux.

2.1.1 Neutronics

The neutronic model corresponds to the time-independent two-group diffusion equation given by:

$$\left[\nabla \cdot \overline{\overline{D}}(\mathbf{r})\nabla + \overline{\overline{\Sigma}}_{sta}(\mathbf{r})\right] \times \begin{bmatrix} \phi_1(\mathbf{r}) \\ \phi_2(\mathbf{r}) \end{bmatrix} = \overline{\overline{F}}(\mathbf{r}) \times \begin{bmatrix} \phi_1(\mathbf{r}) \\ \phi_2(\mathbf{r}) \end{bmatrix}, \tag{1}$$

where the parameter matrices are defined as:

$$\begin{gathered} \overline{\overline{D}}(\boldsymbol{r}) = \begin{bmatrix} D_1(\boldsymbol{r}) & 0 \\ 0 & D_2(\boldsymbol{r}) \end{bmatrix}, \ \overline{\overline{\Sigma}}_{sta}(\boldsymbol{r}) = \begin{bmatrix} -\Sigma_{a1}(\boldsymbol{r}) - \Sigma_{rem}(\boldsymbol{r}) & 0 \\ \Sigma_{rem}(\boldsymbol{r}) & -\Sigma_{a2}(\boldsymbol{r}) \end{bmatrix}, \\ \overline{\overline{F}}(\boldsymbol{r}) = \begin{bmatrix} -\nu\Sigma_{f1}(\boldsymbol{r}) & -\nu\Sigma_{f2}(\boldsymbol{r}) \\ 0 & 0 \end{bmatrix} \end{gathered} \tag{2}$$

where $\phi_1(\mathbf{r})$ and $\phi_2(\mathbf{r})$ denote the time-independent fast and thermal fluxes, and $D_1(\mathbf{r})$, $D_2(\mathbf{r})$, $\Sigma_{a,1}(\mathbf{r})$, $\Sigma_{a,2}(\mathbf{r})$, $\nu\Sigma_{f,1}(\mathbf{r})$, $\nu\Sigma_{f,2}(\mathbf{r})$, $\Sigma_{rem}(\mathbf{r})$ stand for the static diffusion coefficients in fast/thermal group, absorption cross-section in fast/thermal group, average number emitted per fission event times fission cross-section in fast/thermal group and removal cross-section, respectively.

2.1.2 Thermo-hydraulics

The most general time-independent thermal-hydraulic model can be represented by the local conservation equations of mass, momentum and energy as a function of space, which are represented as follows:

$$\overline{\nabla} \cdot [\rho_m(\mathbf{r})\overline{v}_m(\mathbf{r})] = 0, \tag{3}$$

$$\overline{\nabla} \cdot [\rho_m(\mathbf{r})\overline{v}_m(\mathbf{r}) \otimes \overline{v}_m(\mathbf{r})]$$

$$= \overline{\nabla} \cdot \overline{\overline{\tau}}(\mathbf{r}) - \overline{\nabla} P(\mathbf{r}) + \overline{g} \rho_m(\mathbf{r}), \tag{4}$$

$$\overline{\nabla} \cdot [\rho_m(\mathbf{r}) \overline{v}_m(\mathbf{r}) h_m(\mathbf{r})] = -\overline{\nabla} \cdot \overline{q}''(\mathbf{r}), \tag{5}$$

where $\rho_m(\mathbf{r})$, $\overline{v}_m(\mathbf{r})$, $h_m(\mathbf{r})$ and $P(\mathbf{r})$ are the moderator density, velocity, enthalpy and pressure, respectively, $\overline{\overline{\tau}}(\mathbf{r})$ is the stress tensor, $\overline{q}''(\mathbf{r})$ is the heat flux and $\overline{g}$ stands for the gravitational constant. The other notations are standard. To simplify the calculations, the local energy conservation equation was replaced by the corresponding local enthalpy conservation equation, where the enthalpy change due to variations in pressure, stresses and volumetric heat production was assumed to be negligible and, therefore, the corresponding terms in the equation were left out. All flow properties are first discretized and then averaged in space on relevant volumes. Such a spatial homogenization of Eqs. (3) - (5) can be written as

$$\int_{V_m} \overline{\nabla} \cdot [\rho_m(\mathbf{r}) \overline{v}_m(\mathbf{r})] dV = 0, \tag{6}$$

$$\int_{V_m} \overline{\nabla} \cdot [\rho_m(\mathbf{r}) \overline{v}_m(\mathbf{r}) \otimes \overline{v}_m(\mathbf{r})] dV$$

$$= \int_{V_m} \overline{\nabla} \cdot \overline{\overline{\tau}}(\mathbf{r}) dV - \int_{V_m} \overline{\nabla} P(\mathbf{r}) dV + \int_{V_m} \overline{g} \rho_m(\mathbf{r}) dV, \tag{7}$$

$$\int_{V_m} \overline{\nabla} \cdot [\rho_m(\mathbf{r}) \overline{v}_m(\mathbf{r}) h_m(\mathbf{r})] = -\int_{V_m} \overline{\nabla} \cdot \overline{q}''(\mathbf{r}) dV, \tag{8}$$

By assuming one-dimensional upward vertical flow, the cross-flow among bundles is neglected (this is a good approximation for a BWR since fuel bundles are usually surrounded by metal boxes and thus are isolated from each other). One then defines the following notations for the volume- and area-averaged quantities:

$$\left\langle X_m \right\rangle = \frac{1}{V_m} \int_{V_m} X_m(\mathbf{r}) dV, \tag{9}$$

$$\left\{ X_m \right\} = \frac{1}{A_m} \int_{A_m} X_m(\mathbf{r}) dS, \tag{10}$$

By neglecting the axial heat flux and taking into account Gauss divergence theorem, Eqs. (6) – (8) can thus be simplified as:

$$A_m \left(\left\{ \rho_m \right\}_0^+ \left\{ v_{z,m} \right\}_0^+ - \left\{ \rho_m \right\}_0^- \left\{ v_{z,m} \right\}_0^- \right) = 0, \tag{11}$$

$$A_m\left(\left\{\rho_m\right\}_0^+\left[\left\{v_{z,m}\right\}_0^+\right]^2-\left\{\rho_m\right\}_0^-\left[\left\{v_{z,m}\right\}_0^-\right]^2\right)$$

$$=-\frac{F_M V_m}{2D_e\rho_l}\left\langle G_m\right\rangle_0^2(i,j,k)-A_m\left[\left\{P_z\right\}_0^+-\left\{P_z\right\}_0^-\right]-gV_m\left\langle\rho_m\right\rangle_0(i,j,k), \tag{12}$$

$$A_m\left(\left\{\rho_m\right\}_0^+\left\{v_m\right\}_0^+\left\{h_m\right\}_0^+-\left\{\rho_m\right\}_0^-\left\{v_m\right\}_0^-\left\{h_m\right\}_0^-\right)=$$

$$-A_m\left\{q''_r\right\}_0, \tag{13}$$

The "0" subscript is an indicator that the variable in question belongs to the static calculation. The i,j,k -indexes denote the spatial position of a moderator node, whereas A_m and V_m denote the cross-sectional area and volume of the node, respectively. The superscripts "$+$" and "$-$" indicate the upper and the lower node interface, F_M is the pressure friction multiplier (factor) defined separately for single and two-phase regions (see next section), D_e is the hydraulic diameter and $\left\langle G_m\right\rangle_0$ corresponds to the total mass flow rate as liquid. In the present study, the size of a thermo-hydraulic node is chosen to be comparable with the size of the corresponding neutronic node. As a result, the total number of thermo-hydraulic nodes is limited to the number of nodes used in commercial codes for BWRs, i.e. $32\times 32\times 27$. In the above equations, the following set of definitions to simplify spatially-averaged quantities was utilized:

$$\left\{v_{z,m}\right\}_0^{\pm}=\frac{\left\{\rho_m v_{z,m}\right\}_0^{\pm}}{\left\{\rho_m\right\}_0^{\pm}}, \tag{14}$$

$$\left[\left\{v_{z,m}\right\}_0^{\pm}\right]^2=\frac{\left\{\rho_m v_{z,m}^2\right\}_0^{\pm}}{\left\{\rho_m\right\}_0^{\pm}}, \tag{15}$$

$$\left\{h_m\right\}_0^{\pm}=\frac{\left\{\rho_m v_{z,m} h_m\right\}_0^{\pm}}{\left\{\rho_m v_{z,m}\right\}_0^{\pm}}, \tag{16}$$

Nevertheless, for practical terms it was assumed that Eq. (15) can be computed just as the square of Eq. (14).

2.2 Modelling strategy

2.2.1 Thermo-hydraulic modelling

The equations for the conservation of mass, momentum and energy were considered for the mixture of the coolant vapor and liquid at all locations in the core, leading to the so-called Homogeneous Equilibrium Model (HEM). Nevertheless, as will be further explained, the calculated slip ratio from the original data coming from commercial core simulators such as POLCA7 (Lindhal, 2007) is employed for a more realistic computation of the mixture coolant density.

The following iterative process for thermal-hydraulic calculations was applied until the convergence was achieved:

i. All the required nodal data of the core are obtained from core simulators. For the sake of demonstrating the feasibility of the methodology, Ringhals-1 data (cycle 26, 904 EFPH (Hernández-Solís A., et.al., 2011)) were fully available by means of the POLCA7 core simulator. First, the neutronic calculation is performed via CORE SIM, where the aim is to obtain the nodal power of the core.
ii. Once the nodal power is obtained, the nodal enthalpy is calculated using the energy equation (Eq. (13)). During the first iteration, all the core nodes are assumed to have the core outlet pressure and, along with the inlet enthalpy and mass flow rate, these are obtained directly from POLCA7.
iii. By assuming saturation conditions at all nodes, the nodal quality is calculated using the following expression:

$$\left\langle x \right\rangle_0 = \frac{\left\langle h_m \right\rangle_0 - h_l}{h_v - h_l}, \tag{17}$$

Therefore, the nodal void fraction can be computed such as:

$$\left\langle \alpha \right\rangle_0 = \frac{1}{1 + \dfrac{1 - \left\langle x \right\rangle_0}{\left\langle x \right\rangle_0} \dfrac{\rho_v}{\rho_l} s}, \tag{18}$$

The slip ratio s can be calculated from the original POLCA7 data, and it is used to avoid over prediction of the nodal void fraction by using solely the Homogeneous Equilibrium Model. Thus, the coolant density is estimated and updated as a function of the void fraction, i.e.:

$$\left\langle \rho_m \right\rangle_0 = \left\langle \alpha \right\rangle_0 \rho_v + \left(1 - \left\langle \alpha \right\rangle_0\right) \rho_l, \tag{19}$$

iv. Once the density is known, the nodal pressure can be estimated. To estimate the friction pressure drop, the friction factor should be estimated a-priori. In this methodology, the friction pressure drop is computed with the use of the friction multiplier F_M:

$$\left\langle \delta P_z \right\rangle_0 = F_M \frac{V_m \left\langle G_m \right\rangle_0^2}{2 D_e \rho_l}, \tag{20}$$

with F_M defined as:

$$F_M = f_{lo} \varphi_{lo}^2, \tag{21}$$

where the index lo indicates the two-phase flow considered as liquid, f_{lo} is the single-phase Fanning friction factor and φ_{lo} is the two-phase multiplier which is unity in the single phase region. The single-phase friction factor is based on the McAdams correlation (Rust, 1979), which is given by:

$$f_{lo} = \frac{0.184}{\mathrm{Re}^{0.2}}, \quad 3 \cdot 10^4 < \mathrm{Re} < 2 \cdot 10^6 \tag{22}$$

and the two-phase multiplier φ_{lo} is based on the Chisholm correlation (Chisholm, 1973; Shah et.al., 2003).

v. Points i-iv are repeated until the pressure reaches a desired convergence.

2.2.2 Neutronic/thermo hydraulic coupled methodology

In order to have a fully integrated neutronic/thermo-hydraulic tool, a nodal cross-section model that updates the macroscopic cross-sections due to changes on the thermal-hydraulic variables is required. This is illustrated in *Fig. 1*

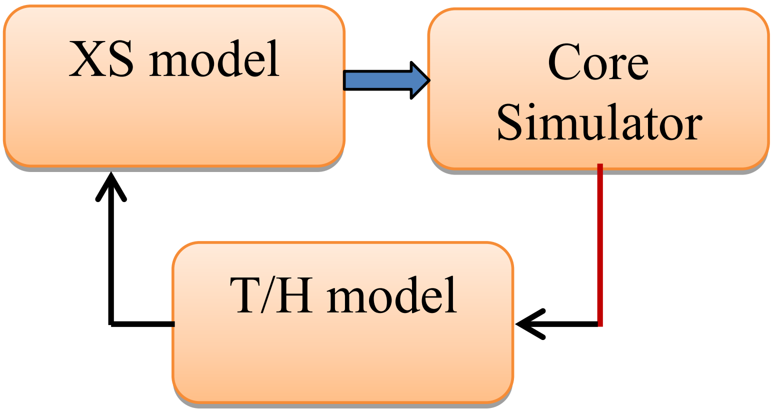

Fig. 1 Neutronic/thermo-hydraulic interaction in a LWR

The cross-section model that was employed for this test case corresponded to the Westinghouse CROSS code (Forslund, 2009), which is the cross-section model embedded in POLCA7 but that may be used as a stand-alone tool. The diagram of *Fig. 1* was implemented until both neutronic convergence (via the nodal neutron flux) and thermal-hydraulic convergence (via the core total pressure drop) are achieved.

2.3 Results of the static calculations

After 4 iterations of the coupled tool, the axial distribution (radially averaged) of the thermal flux and the coolant density are shown in *Fig. 2* and *Fig. 3,* respectively. At each figure, a comparison of the coupled tool is done to the original POLCA7 data in order to validate the implemented modelling strategy.

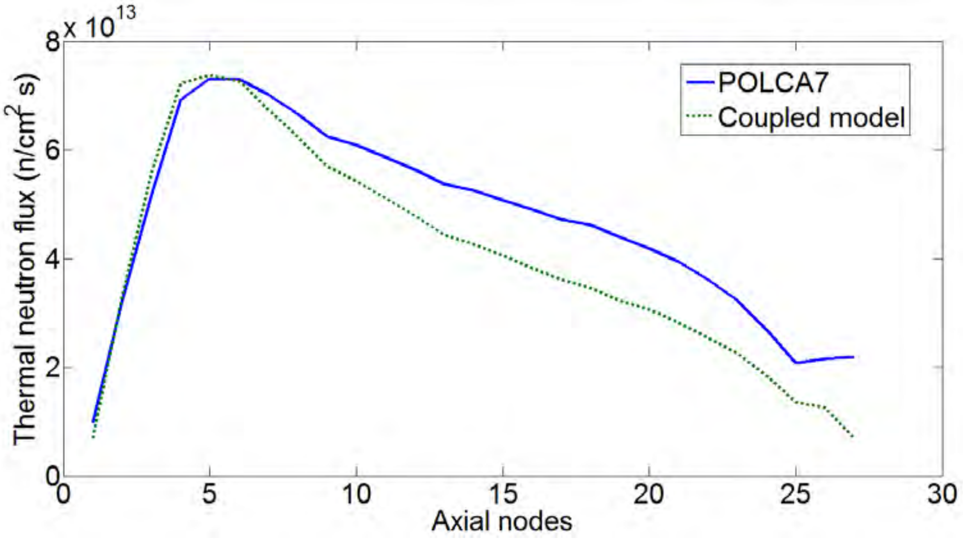

Fig. 2 Axial core thermal flux

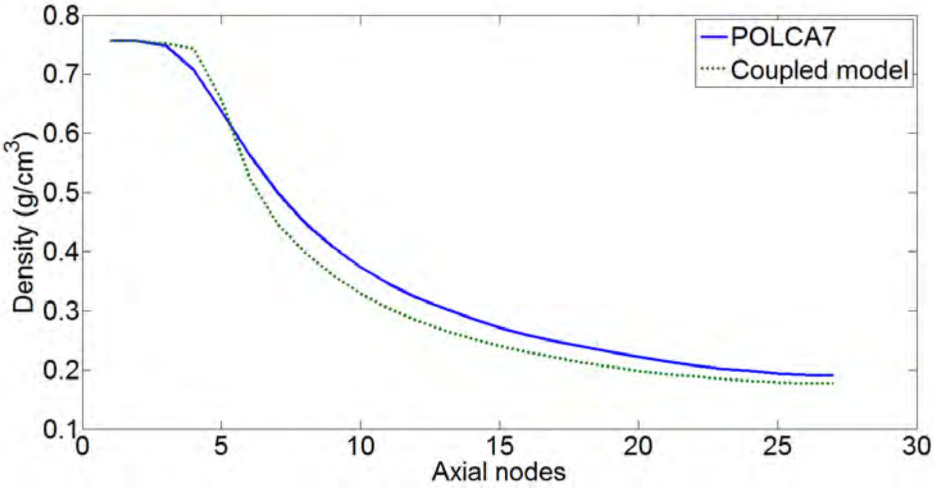

Fig. 3 Axial core coolant density

3 Dynamic calculations

3.1 Derivation of noise equations

In this section, the methodology applied to derive the governing equations for the fluctuations in neutronic and thermo-hydraulic quantities is described. The derivation is performed starting with an application of first order perturbation theory to the time-/space-dependent equations. Here, the main focus is made on the thermo-hydraulic noise equations whereas the derivation of the corresponding neutron noise equations is only touched upon. A more detailed description of the latter topic can be found in (Demazière C. et. al., 2004, 2009, 2011).

3.1.1 Neutronics

A good starting point for deriving the neutron noise equations is the time-/space-dependent two-energy group diffusion equations which in three dimensions are given as:

$$\frac{\partial}{\partial t}\begin{bmatrix}\frac{\phi_1}{v_1}(\mathbf{r},\ t)\\ \frac{\phi_2}{v_2}(\mathbf{r},\ t)\end{bmatrix} = \overline{\nabla}\cdot\begin{bmatrix}D_1(\mathbf{r},\ t) & 0\\ 0 & D_2(\mathbf{r},\ t)\end{bmatrix}\overline{\nabla}\begin{bmatrix}\phi_1(\mathbf{r},t)\\ \phi_2(\mathbf{r},t)\end{bmatrix} - \begin{bmatrix}\Sigma_{a,1}(\mathbf{r},\ t)+\Sigma_{rem}(\mathbf{r},\ t) & 0\\ -\Sigma_{rem}(\mathbf{r},\ t) & \Sigma_{a,2}(\mathbf{r},\ t)\end{bmatrix}\times$$

$$\begin{bmatrix}\phi_1(\mathbf{r},\ t)\\ \phi_2(\mathbf{r},\ t)\end{bmatrix} + (1-\beta_{eff})\frac{1}{k_{eff}}\begin{bmatrix}\nu\Sigma_{f,1}(\mathbf{r},\ t) & \nu\Sigma_{f,2}(\mathbf{r},\ t)\\ 0 & 0\end{bmatrix}\times\begin{bmatrix}\phi_1(\mathbf{r},\ t)\\ \phi_2(\mathbf{r},\ t)\end{bmatrix} + \lambda\begin{bmatrix}1\\ 0\end{bmatrix}C(\mathbf{r},\ t), \quad (23)$$

$$\frac{\partial}{\partial t}C(\mathbf{r},\ t) = \beta_{eff}\frac{1}{k_{eff}}\begin{bmatrix}\nu\Sigma_{f,1}(\mathbf{r},\ t) & \nu\Sigma_{f,2}(\mathbf{r},\ t)\end{bmatrix}\begin{bmatrix}\phi_1(\mathbf{r},\ t)\\ \phi_2(\mathbf{r},\ t)\end{bmatrix} - \lambda C(\mathbf{r},\ t) \quad (24)$$

where $\phi_1(\mathbf{r},\ t)$ and $\phi_2(\mathbf{r},\ t)$ denote the time-dependent fast and thermal fluxes, $C(\mathbf{r},\ t)$ is the concentration of delayed neutron precursors and $D_1(\mathbf{r},\ t)$, $D_2(\mathbf{r},\ t)$, $\Sigma_{a,1}(\mathbf{r},\ t)$, $\Sigma_{a,2}(\mathbf{r},\ t)$, $\nu\Sigma_{f,1}(\mathbf{r},\ t)$, $\nu\Sigma_{f,2}(\mathbf{r},\ t)$, $\Sigma_{rem}(\mathbf{r},\ t)$ stand for time-dependent diffusion coefficients in fast/thermal group, absorption cross-section in fast/thermal group, average number emitted per fission event times fission cross-section in fast/thermal group and removal cross-section, respectively. The other notations are standard.

Next, it is assumed that the small fluctuations of the neutron fluxes $\delta\phi_i(\mathbf{r},\ t)$, $i = 1,2$ around their static (critical) values $\phi_i^0(\mathbf{r})$ i.e.

$$\phi_i(\mathbf{r},\ t) = \phi_i^0(\mathbf{r}) + \delta\phi_i(\mathbf{r},\ t) \quad (25)$$

are given rise by the fluctuations of cross-sections around their static values as:

$$\Sigma_i(\mathbf{r},\ t) = \Sigma_i^0(\mathbf{r}) + \delta\Sigma_i(\mathbf{r},\ t) \quad (26)$$

where $i = a1, a2, f1, f2, rem$ specifies the cross-section type. Following the standard procedure of first order perturbation theory, i.e. substituting Eqs. (25) and (26) into Eqs. (23) and (24), removing static equations, neglecting the second order terms $\delta\phi_i(\mathbf{r},\ t)\delta\Sigma_i(\mathbf{r},\ t)$ and eliminating the concentration of delayed neutron precursors through a Fourier transform, one arrives at the following equations for the fast/thermal neutron noise:

$$-\overline{\nabla}\cdot\begin{bmatrix} D_1^0(\mathbf{r}) & 0 \\ 0 & D_2^0(\mathbf{r}) \end{bmatrix}\overline{\nabla}\begin{bmatrix} \delta\phi_1(\mathbf{r},\ \omega) \\ \delta\phi_2(\mathbf{r},\ \omega) \end{bmatrix} - \begin{bmatrix} \Sigma_{a,1}^0(\mathbf{r}) + \Sigma_{rem}^0(\mathbf{r}) + \frac{\mathrm{I}\omega}{v_1} & 0 \\ -\Sigma_{rem}^0(\mathbf{r}) & \Sigma_{a,2}^0(\mathbf{r}) + \frac{\mathrm{I}\omega}{v_2} \end{bmatrix}\times$$

$$\begin{bmatrix} \delta\phi_1(\mathbf{r},\ \omega) \\ \delta\phi_2(\mathbf{r},\ \omega) \end{bmatrix} + (1 - \frac{\mathrm{I}\omega\beta_{eff}}{\lambda + i\omega})\frac{1}{k_{eff}}\begin{bmatrix} \nu\Sigma_{f,1}^0(\mathbf{r}) & \nu\Sigma_{f,2}^0(\mathbf{r}) \\ 0 & 0 \end{bmatrix}\times\begin{bmatrix} \delta\phi_1(\mathbf{r},\ \omega) \\ \delta\phi_2(\mathbf{r},\ \omega) \end{bmatrix} = \begin{bmatrix} \delta S_1(\mathbf{r},\ \omega) \\ \delta S_2(\mathbf{r},\ \omega) \end{bmatrix}, \quad (27)$$

with the two terms ($\delta S_1(\boldsymbol{r},\omega)$ and $\delta S_2(\boldsymbol{r},\omega)$) on the right hand side standing for the neutron noise sources in the fast and thermal groups, respectively and defined as:

$$\begin{bmatrix} \delta S_1(\mathbf{r},\ \omega) \\ \delta S_2(\mathbf{r},\ \omega) \end{bmatrix} = \begin{bmatrix} -\delta\Sigma_{rem}(\mathbf{r},\ \omega)\times\phi_1^0(\mathbf{r}) \\ \delta\Sigma_{rem}(\mathbf{r},\ \omega)\times\phi_1^0(\mathbf{r}) \end{bmatrix} + \begin{bmatrix} \delta\Sigma_{a,1}(\mathbf{r},\ \omega)\times\phi_1^0(\mathbf{r}) \\ \delta\Sigma_{a,2}(\mathbf{r},\ \omega)\times\phi_2^0(\mathbf{r}) \end{bmatrix} +$$

$$\begin{bmatrix} \sum_{i=1}^{2}\frac{1}{k_{eff}}(1 - \frac{\mathrm{I}\omega\beta_{eff}}{\lambda + \mathrm{I}\omega})\delta\Sigma_{f,i}(\mathbf{r},\ \omega)\times\phi_i^0(\mathbf{r}) \\ 0 \end{bmatrix}, \quad (28)$$

After applying a node-wise spatial discretization based on finite differences, the above equations can be rewritten in the following matrix form:

$$\overline{\overline{M}}(i,j,k,\omega)\times\begin{bmatrix} \delta\phi_1(i,j,k,\omega) \\ \delta\phi_2(i,j,k,\omega) \end{bmatrix} = \begin{bmatrix} \delta S_1(i,j,k,\omega) \\ \delta S_2(i,j,k,\omega) \end{bmatrix}. \quad (29)$$

The system of linear equations (29) can be solved for the neutron noise $\delta\phi_1(i,j,k,\omega)$ and $\delta\phi_2(i,j,k,\omega)$ by using standard Gaussian elimination. Another way to obtain the same solution would be to apply Greens function method which then requires the computationally-intensive inversion of the matrix. For more details one refers to (Demazière C. et. al., 2011).

As Eqs. (27)-(29) show, the calculation of the neutron noise requires an explicit modelling of the neutron noise sources, i.e. the driving perturbations in the cross-sections which so far have been left undetermined. In general, these perturbations are usually induced by the fluctuations in the corresponding thermo-hydraulic parameters, in particular, by the fluctuations in moderator density and fuel temperature. The modelling of such perturbations will then be discussed separately in one of the consecutive sections (see Section 3.1.4).

3.1.2 Thermo-hydraulics

In order to derive the driving equations for the thermo-hydraulic noise, the same approach as described in the previous section is applied, i.e. starting with the local time-/space-dependent mass, momentum and energy conservation equations given as:

$$\frac{\partial}{\partial t}\rho_m(\mathbf{r},\ t) + \overline{\nabla}\cdot[\rho_m(\mathbf{r},\ t)\overline{v}_m(\mathbf{r},\ t)] = 0, \tag{30}$$

$$\frac{\partial}{\partial t}[\rho_m(\mathbf{r},\ t)\overline{v}_m(\mathbf{r},\ t)] + \overline{\nabla}\cdot[\rho_m(\mathbf{r},\ t)\overline{v}_m(\mathbf{r},\ t)\otimes\overline{v}_m(\mathbf{r},\ t)]$$

$$= \overline{\nabla}\cdot\overline{\overline{\tau}}(\mathbf{r},\ t) - \overline{\nabla}P(\mathbf{r},\ t) + \overline{g}\rho_m(\mathbf{r},\ t), \tag{31}$$

$$\frac{\partial}{\partial t}[\rho_m(\mathbf{r},\ t)h_m(\mathbf{r},\ t)] + \overline{\nabla}\cdot[\rho_m(\mathbf{r},\ t)\overline{v}_m(\mathbf{r},\ t)h_m(\mathbf{r},\ t)] = -\overline{\nabla}\cdot\overline{q}''(\mathbf{r},\ t). \tag{32}$$

Here, we utilize the same set of approximations and notations as introduced in the static thermo-hydraulic equations. Since the full microscopic description of the two-phase flow is generally not possible (i.e. Eqs. (30)-(32) cannot be solved in both time and space in an exact manner), another technique, referred to as a “macroscopic description” is usually used. In such a case, all flow properties are discretized and then averaged in space on the relevant space volumes. The spatial homogenization of Eqs. (30)-(32) is written as:

$$\frac{\partial}{\partial t}\int_{V_m}\rho_m(\mathbf{r},\ t)dV + \int_{V_m}\overline{\nabla}\cdot[\rho_m(\mathbf{r},\ t)\overline{v}_m(\mathbf{r},\ t)]dV = 0, \tag{33}$$

$$\frac{\partial}{\partial t}\int_{V_m}[\rho_m(\mathbf{r},\ t)\overline{v}_m(\mathbf{r},\ t)]dV + \int_{V_m}\overline{\nabla}\cdot[\rho_m(\mathbf{r},\ t)\overline{v}_m(\mathbf{r},\ t)\otimes\overline{v}_m(\mathbf{r},\ t)]dV$$

$$= \int_{V_m}\overline{\nabla}\cdot\overline{\overline{\tau}}(\mathbf{r},\ t)dV - \int_{V_m}\overline{\nabla}P(\mathbf{r},\ t)dV + \int_{V_m}\overline{g}\rho_m(\mathbf{r},\ t)dV, \tag{34}$$

$$\frac{\partial}{\partial t}\int_{V_m}[\rho_m(\mathbf{r},\ t)h_m(\mathbf{r},\ t)]dV + \int_{V_m}\overline{\nabla}\cdot[\rho_m(\mathbf{r},\ t)\overline{v}_m(\mathbf{r},\ t)h_m(\mathbf{r},\ t)] = -\int_{V_m}\overline{\nabla}\cdot\overline{q}''(\mathbf{r},\ t)dV, \tag{35}$$

Then, introducing the following notations for the volume- and area-averaged quantities:

$$\left\langle X_m\right\rangle(t) = \frac{1}{V_m}\int_{V_m}X_m(\mathbf{r},t)dV, \tag{36}$$

$$\left\{X_m\right\}(t) = \frac{1}{A_m}\int_{A_m}X_m(\mathbf{r},t)dS, \tag{37}$$

assuming one-dimensional upward vertical flow and taking into account Gauss divergence theorem, Eqs. (33)-(34) can be simplified as:

$$V_m \frac{\partial}{\partial t}\left\langle \rho_m \right\rangle (i,j,k,t) + A_m \left(\left\{ \rho_m \right\}^+ \left\{ v_{z,m} \right\}^+ (t) - \left\{ \rho_m \right\}^- \left\{ v_{z,m} \right\}^- (t) \right) = 0, \tag{38}$$

$$V_m \frac{\partial}{\partial t}\left\langle \rho_m \right\rangle \left\langle v_{z,m} \right\rangle (i,j,k,t) + A_m \left(\left\{ \rho_m \right\}^+ \left[\left\{ v_{z,m} \right\}^+ \right]^2 (t) - \left\{ \rho_m \right\}^- \left[\left\{ v_{z,m} \right\}^- \right]^2 (t) \right) =$$

$$-\frac{F_M V_m}{2 D_e \rho_l} \left\langle \rho_m \right\rangle^2 \left\langle v_m \right\rangle^2 (i,j,k,t) - A_m \left[\left\{ P_m \right\}^+ (t) - \left\{ P_m \right\}^- (t) \right] - g V_m \left\langle \rho_m \right\rangle (i,j,k,t), \tag{39}$$

$$V_m \frac{\partial}{\partial t}\left\langle \rho_m \right\rangle \left\langle h_m \right\rangle (i,j,k,t) + A_m \left(\left\{ \rho_m \right\}^+ \left\{ v_{z,m} \right\}^+ \left\{ h_m \right\}^+ - \left\{ \rho_m \right\}^- \left\{ v_{z,m} \right\}^- \left\{ h_m \right\}^- \right) =$$

$$-A_m \left\{ q_r'' \right\} (t). \tag{40}$$

In the above equations, the following set of additional definitions and approximations compared to the static case (see Eqs. (14)-(16)) was utilized:

$$\left\langle v_{z,m} \right\rangle (i,j,k,t) = \frac{\left\langle \rho_m v_{z,m} \right\rangle (i,j,k,t)}{\left\langle \rho_m \right\rangle (i,j,k,t)}, \tag{41}$$

$$\left\langle h_m \right\rangle (i,j,k,t) = \frac{\left\langle \rho_m h_m \right\rangle (i,j,k,t)}{\left\langle \rho_m \right\rangle (i,j,k,t)}. \tag{42}$$

$$\left\{ h_m \right\}^\pm (t) = \frac{\left\{ \rho_m h_m \right\}^\pm (t)}{\left\{ \rho_m \right\}^\pm (t)}, \tag{43}$$

$$\left\{ \hat{h}_m \right\}^\pm (t) = \frac{\left\{ \rho_m v_{z,m} h_m \right\}^\pm (t)}{\left\{ \rho_m v_{z,m} \right\}^\pm (t)}. \tag{44}$$

In the above calculations, it was assumed that $\left\{ \hat{h}_m \right\}_0^\pm \approx \left\{ h_m \right\}^\pm$. It should be underlined that the term on the right-hand side of equation (40) requires a special treatment, namely it should be expressed through the known quantities. For this purpose, it is assumed that all radial heat produced in the fuel region of an assembly (or node) is directly transferred into the coolant region as:

$$\left\{ q_r'' \right\}_f (t) = -\left\{ q_r'' \right\}_{\mathrm{m}} (t). \tag{45}$$

Using Fourier's law of conduction written as:

$$\overline{q}''(\mathbf{r}, t) = -k_f(T_f)\overline{\nabla} T_f(\mathbf{r}, t) \tag{46}$$

the area-averaged heat flux in the fuel region can be approximated as:

$$\left\{q_r''\right\}_f(t) \approx H_0\left(\left\langle T_f\right\rangle(i,j,k,t)-\left\langle T_m\right\rangle(i,j,k,t)\right), \tag{47}$$

where H_0 stands for the artificial static heat transfer coefficient (H_0 differs from the real one since one doesn't use the wall temperature). Combining Eqs. (45) and (47) for the heat flux in the moderator region, one gets:

$$\left\{q_r''\right\}_{\mathrm{m}}(t) = H_0(\left\langle T_f\right\rangle(i,j,k,t)-\left\langle T_m\right\rangle(i,j,k,t)). \tag{48}$$

To obtain the equations for the fluctuations, the same procedure (i.e. first order perturbation theory) as for the neutron noise, is applied, i.e. splitting all time-dependent quantities in Eqs. (38)-(40) into their mean values and fluctuating parts as:

$$\left\{X_m\right\}^{\pm}(t) = \left\{X_m\right\}_0^{\pm} + \left\{\delta X_m\right\}^{\pm}(t), \tag{49}$$

$$\left\langle X_m\right\rangle(i,j,k,t) = \left\langle X_m\right\rangle_0(i,j,k) + \left\langle \delta X_m\right\rangle(i,j,k,t), \tag{50}$$

neglecting the second order terms, subtracting static equations, performing a Fourier transform and assuming the following approximate relation between the area-averaged and the volume-averaged values:

$$\left\langle X_m\right\rangle(i,j,k,t) = \frac{\left\{X_m\right\}^{+}(t)+\left\{X_m\right\}^{-}(t)}{2}, \tag{51}$$

with X_m designating any thermo-hydraulic quantity, the noise equations for calculating the thermo-hydraulic fluctuations read as:

$$V_m \mathrm{I}\omega\left\langle\delta\rho_m\right\rangle(i,j,k,\omega) + A_m\left(\left\{\delta\rho_m\right\}^{+}(\omega)\left\{v_{z,m}\right\}_0^{+} - \left\{\delta\rho_m\right\}^{-}(\omega)\left\{v_{z,m}\right\}_0^{-}\right) +$$
$$A_m\left(\left\{\rho_m\right\}_0^{+}\left\{\delta v_{z,m}\right\}^{+}(\omega) - \left\{\rho_m\right\}_0^{-}\left\{\delta v_{z,m}\right\}^{-}(\omega)\right) = 0, \tag{52}$$

$$\frac{V_m \mathrm{I}\omega}{2}\left(\left\langle\rho_m\right\rangle_0(i,j,k)\left\{\delta v_{z,m}\right\}^{+}(t) + \left\langle\rho_m\right\rangle_0(i,j,k)\left\{\delta v_{z,m}\right\}^{-}(t) + \left\{\delta\rho_m\right\}^{+}(t)\left\langle v_{z,m}\right\rangle_0(i,j,k)\right) +$$

$$\frac{V_m \mathrm{I}\omega}{2}\left\{\delta\rho_m\right\}^{-}(t)\left\langle v_{z,m}\right\rangle_0(i,j,k) + A_m\left(\left\{\delta\rho_m\right\}^{+}(t)\left[\left\{v_{z,m}\right\}_0^{+}\right]^2(i,j,k)\right) +$$

$$A_m\left(2\left\{\rho_m\right\}_0^{+}\left\{v_{z,m}\right\}_0^{+}(i,j,k)\left\{\delta v_{z,m}\right\}^{+}(t) - \left\{\delta\rho_m\right\}^{-}(t)\left[\left\{v_{z,m}\right\}_0^{-}\right]^2(i,j,k)\right) -$$

$$-2A_m\left\{\rho_m\right\}_0^{-}\left\{v_m\right\}_0^{-}(i,j,k)\left\{\delta v_{z,m}\right\}^{-}(t) + \frac{F_M V_m}{4D_e\rho_l}\left\langle G_m\right\rangle_0(i,j,k)\left\{\delta\rho_m\right\}^{+}(t)\left\langle v_{z,m}\right\rangle_0(i,j,k) +$$

$$\frac{F_M V_m}{2D_e\rho_l}\left\langle G_m\right\rangle_0(i,j,k)\left(\left\{\delta\rho_m\right\}^{-}(t)\left\langle v_{z,m}\right\rangle_0(i,j,k) + \left\langle\rho_m\right\rangle_0\left\{\delta\hat{v}_{z,m}\right\}^{-}(t)\right) +$$

$$\frac{F_M V_m}{4D_e\rho_l}\left\langle G_m\right\rangle_0\left\langle \rho_m\right\rangle_0(i,j,k)\left\{\delta v_{z,m}\right\}^+(t)+A_m\left[\left\{\delta P_m\right\}^+(t)-\left\{\delta P_m\right\}^-(t)\right]+$$

$$\frac{gV_m}{2}\left(\left\{\delta\rho_m\right\}^+(t)+\left\{\delta\rho_m\right\}^-(t)\right)=0, \tag{53}$$

$$\frac{V_m \mathrm{I}\omega}{2}\left(\left\langle \hat{h}_m\right\rangle_0(i,j,k)\left[\left\{\delta\rho_m\right\}^+(t)+\left\{\delta\rho_m\right\}^-(t)\right]+\left\langle \rho_m\right\rangle_0(i,j,k)\left[\left\{\delta h_m\right\}^+(t)+\left\{\delta h_m\right\}^-(t)\right]\right)+$$

$$A_m\left(\left\{h_m\right\}_0^+\left\{\rho_m\right\}_0^+\left\{\delta v_{z,m}\right\}^+(t)+\left\{h_m\right\}_0^+\left\{\delta\rho_m\right\}^+(t)\left\{v_{z,m}\right\}_0^+ +\left\{\delta h_m\right\}^+(t)\left\{\rho_m\right\}_0^+\left\{v_{z,m}\right\}_0^+\right)-$$

$$A_m\left(\left\{h_m\right\}_0^-\left\{\rho_m\right\}_0^-\left\{\delta v_{z,m}\right\}^-(t)+\left\{h_m\right\}_0^-\left\{\delta\rho_m\right\}^-(t)\left\{v_{z,m}\right\}_0^- +\left\{\delta h_m\right\}^-(t)\left\{\rho_m\right\}_0^-\left\{v_{z,m}\right\}_0^-\right)=$$

$$V_m H_{eff}\left(\left\langle \delta T_f\right\rangle(t)-\left\langle \delta T_m\right\rangle(t)\right). \tag{54}$$

where H_{eff} is the effective heat transfer coefficient. Equations (52)-(54) are then used to calculate the fluctuations in moderator density, velocity and pressure. More details on such calculations will be given below.

3.1.3 Heat transfer

To derive the equations describing the noise in fuel temperature, we follow the same methodology as was implemented in the previous two sections, namely starting with local time -and space-dependent heat balance equation written as:

$$\rho_f(T_f)c_f(T_f)\frac{\partial}{\partial t}T_f(\mathbf{r},t)=\overline{\nabla}\cdot\overline{q}''(\mathbf{r},t)+q'''(\mathbf{r},t). \tag{55}$$

Integrating both sides of Eq.(55) over the fuel volume, one obtains

$$\rho_f(T_f)c_f(T_f)\frac{\partial}{\partial t}\int_{V_f}T_f(\mathbf{r},t)dV=\int_{V_f}\overline{\nabla}\cdot\overline{q}''(\mathbf{r},t)dV+\int_{V_f}q'''(\mathbf{r},t)dV. \tag{56}$$

Introducing the following notations for the volume and area-averaged quantities in the fuel region:

$$\left\langle X_f\right\rangle(t)=\frac{1}{V_f}\int_{V_f}X_f(\mathbf{r},t)dV, \tag{57}$$

$$\left\{X_f\right\}(t)=\frac{1}{A_f}\int_{A_f}X_f(\mathbf{r},t)dS, \tag{58}$$

and approximating the averaged heat flux as:

$$\int_{V_f}\overline{\nabla}\cdot\overline{q}''(\mathbf{r},t)dV\approx\int_{S_f}q_r''(\mathbf{r},t)dS=S_f\left\{q_r''\right\}_f(t), \tag{59}$$

Eq. (55) reads as:

$$\rho_f(T_f)c_f(T_f)V_f\frac{\partial}{\partial t}\left\langle T_f\right\rangle(i,j,k,t)=S_f\left\{q_r''\right\}_f(t)+V_f\left\langle q'''\right\rangle(i,j,k,t). \tag{60}$$

Combining Eq. (47) with Eq. (60), one obtains the following time-space dependent equation describing the evolution of the fuel temperature:

$$\rho_f(T_f)c_f(T_f)\frac{\partial}{\partial t}\left\langle T_f\right\rangle(i,j,k,t)=H_{eff}\left(\left\langle T_f\right\rangle(i,j,k,t)-\left\langle T_m\right\rangle(i,j,k,t)\right)+\left\langle q'''\right\rangle(i,j,k,t). \tag{61}$$

Finally, after the application of first order perturbation theory (similarly to the previous two cases), the equation for the noise in fuel temperature can be written as

$$\rho_f c_f \mathrm{I}\omega\left\langle\delta T_f\right\rangle(i,j,k,\omega)=-H_{eff}\left(\left\langle\delta T_f\right\rangle(i,j,k,\omega)-\left\langle\delta T_m\right\rangle(i,j,k,\omega)\right)+\left\langle\delta q'''\right\rangle(i,j,k,\omega). \tag{62}$$

3.1.4 Additional correlations

The thorough analysis of the above equations shows that this set of noise equations is not fully closed, i.e. the number of unknown quantities exceeds the number of available equations. Therefore, additional correlations between different thermo-hydraulic parameters as well as between thermo-hydraulic and neutronic parameters are needed and will be specified in this section. Such correlations will then help to simplify the corresponding set of equations as well as to reduce the number of unknown parameters to be directly solved for.

- Thermo-hydraulic correlations

First, it is assumed that the enthalpy fluctuations can be represented as a linear combination of the fluctuations in pressure and density, i.e. in the following form:

$$\left\{\delta h_m\right\}^{\pm}(\omega)=\alpha^{\pm}\left\{\delta P_m\right\}^{\pm}(\omega)+\beta^{\pm}\left\{\delta\rho_m\right\}^{\pm}(\omega), \tag{63}$$

where the coefficient $\alpha^{\pm}$ and $\beta^{\pm}$ stand for the enthalpy derivatives with the respect to pressure and density and defined correspondingly as:

$$\alpha^{\pm}=\left.\frac{\partial\left\{h_m\right\}^{\pm}}{\partial\left\{P_{z,m}\right\}^{\pm}}\right|_{\left\{\rho_m\right\}^{\pm}=const}=\left.\frac{dh_l^{\pm}}{dP_m^{\pm}}\right|_{\left\{\hat{\rho}_m\right\}^{\pm}=const}+\rho_v^{\pm}s^{\pm}\left(\left.\frac{dh_v^{\pm}}{dP_m^{\pm}}\right|_{\left\{\rho_m\right\}^{\pm}=const}-\left.\frac{dh_l^{\pm}}{dP_m^{\pm}}\right|_{\left\{\rho_m\right\}^{\pm}=const}\right)\times$$

$$\left(\frac{\left\{\rho_m\right\}_0^{\pm}-\rho_l^{\pm}}{\rho_l^{\pm}\rho_v^{\pm}\left(1-s^{\pm}\right)+\left\{\rho_m\right\}_0^{\pm}\left(s^{\pm}\rho_v^{\pm}-\rho_l^{\pm}\right)}\right)+\left(h_v^{\pm}-h_l^{\pm}\right)\rho_v^{\pm}s^{\pm}\left(-\frac{\left.\frac{d\rho_l^{\pm}}{d\left\{P_m\right\}^{\pm}}\right|_{\left\{\rho_m\right\}^{\pm}=const}}{\rho_l^{\pm}\rho_v^{\pm}\left(1-s^{\pm}\right)+\left\{\hat{\rho}_m\right\}_0^{\pm}\left(s^{\pm}\rho_v^{\pm}-\rho_l^{\pm}\right)}\right.$$

$$\frac{\left(\left\{\rho_m\right\}_0^{\pm}-\rho_l^{\pm}\right)}{\rho_l^{\pm}\rho_v^{\pm}\left(1-s^{\pm}\right)+\left\{\rho_m\right\}_0^{\pm}\left(s^{\pm}\rho_v^{\pm}-\rho_v^{\pm}\right)}\left(\rho_v^{\pm}\left(1-s^{\pm}\right)\frac{d\rho_l^{\pm}}{d\left\{P_m\right\}^{\pm}}\Bigg|_{\left\{\rho_m\right\}^{\pm}=const}+\rho_l^{\pm}\left(1-s^{\pm}\right)\times\right.$$

$$\left.\left.\frac{d\rho_v^{\pm}}{d\left\{P_m\right\}^{\pm}}\Bigg|_{\left\{\rho_m\right\}^{\pm}=const}+\left\{\rho_m\right\}_0^{\pm}\left(s^{\pm}\frac{d\rho_v^{\pm}}{d\left\{P_m\right\}^{\pm}}\Bigg|_{\left\{\rho_m\right\}^{\pm}=const}-\frac{d\rho_l^{\pm}}{d\left\{P_m\right\}^{\pm}}\Bigg|_{\left\{\rho_m\right\}^{\pm}=const}\right)\right)\right)+$$

$$s^{\pm}\frac{d\rho_v^{\pm}}{d\left\{P_m\right\}^{\pm}}\Bigg|_{\left\{\rho_m\right\}^{\pm}=const}\frac{\left(h_v^{\pm}-h_l^{\pm}\right)\left(\left\{\hat{\rho}_m\right\}_0^{\pm}-\rho_l^{\pm}\right)}{\rho_l^{\pm}\rho_v^{\pm}\left(1-s^{\pm}\right)+\left\{\hat{\rho}_m\right\}_0^{\pm}\left(s^{\pm}\rho_v^{\pm}-\rho_l^{\pm}\right)}, \tag{64}$$

$$\beta^{\pm}=\frac{\partial\left\{h_m\right\}^{\pm}}{\partial\left\{\rho_m\right\}^{\pm}}\Bigg|_{\left\{P_m\right\}^{\pm}=const}=\frac{s^{\pm}\rho_v^{\pm}\rho_l^{\pm}\left(h_v^{\pm}-h_l^{\pm}\right)\left(\rho_v^{\pm}-\rho_l^{\pm}\right)}{\left(\rho_l^{\pm}\rho_v^{\pm}\left(1-s^{\pm}\right)+\left\{\rho_m\right\}_0^{\pm}\left(s^{\pm}\rho_v^{\pm}-\rho_l^{\pm}\right)\right)^2}, \tag{65}$$

where $s^{\pm}$ is the interfacial slip ration, $\rho_l^{\pm}$, $\rho_v^{\pm}$, $h_l^{\pm}$ and $h_v^{\pm}$ are saturated density and enthalpy of the liquid and vapour phases taken at the interfaces of the nodes, respectively, and their corresponding derivatives calculated from water tables at steady-state conditions are defined as:

$$\frac{d\rho_l^{\pm}}{d\left\{P_m\right\}^{\pm}}\Bigg|_{\left\{\rho_m\right\}^{\pm}=const}=\frac{\delta\rho_l^{\pm}}{\delta\left\{P_m\right\}^{\pm}}\Bigg|_{\left\{\rho_m\right\}^{\pm}=const} \tag{66}$$

$$\frac{d\rho_v^{\pm}}{d\left\{P_m\right\}^{\pm}}\Bigg|_{\left\{\rho_m\right\}^{\pm}=const}=\frac{\delta\rho_v^{\pm}}{\delta\left\{P_m\right\}^{\pm}}\Bigg|_{\left\{\rho_m\right\}^{\pm}=const} \tag{67}$$

$$\frac{dh_l^{\pm}}{d\left\{P_m\right\}^{\pm}}\Bigg|_{\left\{\rho_m\right\}^{\pm}=const}=\frac{\delta h_l^{\pm}}{\delta\left\{P_m\right\}^{\pm}}\Bigg|_{\left\{\rho_m\right\}^{\pm}=const} \tag{68}$$

$$\frac{dh_v^{\pm}}{d\left\{P_m\right\}^{\pm}}\Bigg|_{\left\{\rho_m\right\}^{\pm}=const}=\frac{\delta h_v^{\pm}}{\delta\left\{P_m\right\}^{\pm}}\Bigg|_{\left\{\rho_m\right\}^{\pm}=const} \tag{69}$$

In general, the explicit expressions for the respective derivatives $\alpha^{\pm}$ and $\beta^{\pm}$ can be obtained from the following generic equation (derived from Eqs. (17)-(19) written for dynamic quantities):

$$\left\{h_m\right\}^{\pm} = h_l^{\pm} + \frac{\left(h_v^{\pm} - h_l^{\pm}\right)\left(\left\{\rho_m\right\}_0^{\pm} - \rho_l^{\pm}\right)\rho_v^{\pm} s^{\pm}}{\rho_l^{\pm}\rho_v^{\pm}\left(1 - s^{\pm}\right) + \left\{\rho_m\right\}_0^{\pm}\left(s^{\pm}\rho_v^{\pm} - \rho_l^{\pm}\right)} \tag{70}$$

by taking the partial derivatives w.r.t. pressure or density. The complexity of such expressions is mainly due to the presence of two phases where the drift flux model or slip model is needed to be applied. However, for the single phase region, Eq.(64)-(65) can be simplified as:

$$\alpha^{\pm} = \left.\frac{\partial\left\{h_m\right\}^{\pm}}{\partial\left\{P_m\right\}^{\pm}}\right|_{\left\{\rho_m\right\}^{\pm}=const} \approx \left.\frac{\delta\left\{h_m\right\}^{\pm}}{\delta\left\{P_m\right\}^{\pm}}\right|_{\left\{\rho_m\right\}^{\pm}=const}, \tag{71}$$

$$\beta^{\pm} = \left.\frac{\partial\left\{h_m\right\}^{\pm}}{\partial\left\{P_m\right\}^{\pm}}\right|_{\left\{\rho_m\right\}^{\pm}=const} \approx \left.\frac{\delta\left\{h_m\right\}^{\pm}}{\delta\left\{P_m\right\}^{\pm}}\right|_{\left\{\rho_m\right\}^{\pm}=const}. \tag{72}$$

Further, a similar linear approximation is applied to model the fluctuations in the moderator temperature which, as in the case of enthalpy, is assumed to be a function of pressure and density and thus can be expressed as:

$$\left\{\delta T_m\right\}^{\pm}(t) = \gamma^{\pm}\left\{\delta\rho_m\right\}^{\pm}(t) + \theta^{\pm}\left\{\delta P_m\right\}^{\pm}(t), \tag{73}$$

where the coefficients $\gamma^{\pm}$ and $\theta^{\pm}$ representing the respective derivatives of the moderator temperature w.r.t. pressure and density given as:

$$\gamma^{\pm} = \left.\frac{\partial\left\{T_m\right\}^{\pm}}{\partial\left\{\rho_m\right\}^{\pm}}\right|_{\left\{P_m\right\}^{\pm}=const} = \left.\frac{\delta\left\{T_m\right\}^{\pm}}{\delta\left\{\rho_m\right\}^{\pm}}\right|_{\left\{P_m\right\}^{\pm}=const}, \tag{74}$$

$$\theta^{\pm} = \left.\frac{\partial\left\{T_m\right\}^{\pm}}{\partial\left\{P_m\right\}^{\pm}}\right|_{\left\{\rho_m\right\}^{\pm}=const} = \left.\frac{\delta\left\{T_m\right\}^{\pm}}{\delta\left\{P_m\right\}^{\pm}}\right|_{\left\{\rho_m\right\}^{\pm}=const}. \tag{75}$$

$\gamma^{\pm}$ and $\theta^{\pm}$ are again estimated from thermo-hydraulic tables at the steady-state conditions. Since the moderator temperature becomes constant in two phase region , i.e. it is equal to the saturation temperature, $\gamma^{\pm}$ and $\theta^{\pm}$ are calculated only for the single phase region and are assumed to be zero otherwise. It should be also underlined, that all linear coefficients $\alpha^{\pm}$, $\beta^{\pm}$, $\gamma^{\pm}$ and $\theta^{\pm}$ are calculated for each node separately and thus are unique. The estimations of these coefficients are performed with the help of water tables by introducing a small 1% (from the respective node-wise mean value) perturbation, whether in pressure for constant density or in density for constant pressure and then evaluating the induced fluctuation in enthalpy or moderator temperature.

Here, it should be pointed out that the assumed linear dependence between fluctuations in enthalpy/moderator temperature and the ones in pressure/density is valid only for small stationary fluctuations and can not be applied to non-stationary or transient conditions. In the present study, where first-order perturbation theory is utilized, such an assumption of linearity holds rather well. In addition, for stationary processes, the dependence between enthalpy and moderator temperature on pressure and density can be assumed quite smooth, thus justifying the assumption mentioned above.

- Neutronic/thermo-hydraulic correlations:

As earlier mentioned in one of the previous sections, in order to calculate the neutron noise, the corresponding neutron noise source should explicitly be given. Conventionally, in neutron noise theory, the respective noise source is often represented as a perturbation in the respective cross-section(s). In its turn, the neutron cross-sections are usually the function of two thermo-hydraulic quantities, i.e. density and fuel temperature. As a result of this dependence, any perturbation in thermo-hydraulic parameters will lead to the corresponding perturbation in cross-sections, creating the noise source for the fluctuations in neutron density. Thus, using a similar linear approach as in the previous case, a fluctuation in any of the cross-sections can be written as a linear combination between two fluctuations: one in fuel temperature and another one in moderator density. From the latter, one gets:

$$\delta \Sigma_X(i,j,k,\omega) \approx \sigma_{i,j,k} \left\langle \delta\rho_m \right\rangle(i,j,k,\omega) + \eta_{i,j,k} \left\langle \delta T_f \right\rangle(i,j,k,\omega), \tag{76}$$

where the index X denotes the cross-section type and the coefficients $\sigma_{i,j,k}$ and $\eta_{i,j,k}$ are the corresponding derivatives of the cross-sections w.r.t. density and fuel temperature, respectively, and defined as:

$$\sigma_{i,j,k} = \left.\frac{\partial \Sigma_X}{\partial \left\langle \rho_m \right\rangle}\right|_{\left\langle T_f \right\rangle = const} \approx \left.\frac{\delta \Sigma_X}{\delta \left\langle \rho_m \right\rangle}\right|_{\left\langle T_f \right\rangle = const}, \tag{77}$$

$$\eta_{i,j,k} = \left.\frac{\partial \Sigma_X}{\partial \left\langle T_f \right\rangle}\right|_{\left\langle \rho_m \right\rangle = const} \approx \left.\frac{\delta \Sigma_X}{\delta \left\langle T_f \right\rangle}\right|_{\left\langle \rho_m \right\rangle = const}. \tag{78}$$

The cross-section derivatives $\sigma_{i,j,k}$ and $\eta_{i,j,k}$ were calculated under steady-state conditions. For this purpose, three separate static simulations were performed. The first simulation was done at steady-state conditions, the second one with a small homogeneous perturbation in the steady-state density ($\delta\left\langle \rho_m \right\rangle = -0.0033$ g/cm^3) for a fixed fuel temperature ($\delta\left\langle T_f \right\rangle = 0$ K) and the last one for a small homogeneous perturbation in the steady-state fuel temperature ($\delta\left\langle T_f \right\rangle = 5$ K) for a fixed moderator density ($\delta\left\langle \rho_m \right\rangle = 0$ g/cm^3). The corresponding changes in the cross-section weighted with the respective perturbations in the density or fuel temperature provided the required values of $\sigma_{i,j,k}$ and $\eta_{i,j,k}$ for each node.

Again, the linear dependence of the cross-sections on thermo-hydraulic parameters, implemented in the above calculations is justified by the fact that only small stationary fluctuations are considered in the present investigation.

3.2 Calculation procedure

This section aims at giving a detailed overview of the calculation procedure used to evaluate the fluctuations in both neutronic and thermo-hydraulic quantities. As a first step, the set of thermo-hydraulic noise equations derived in the previous sections, are solved to obtain explicit expressions for the noise in coolant velocity, moderator density and pressure. Thus, combining Eqs.(52)-(54), (62) with Eqs.(63), (73) one gets:

$$\left\{\delta v_{z,m}\right\}^{+}(\omega) = -\frac{1}{c_{i,j,k}}\left(\left\{\delta\rho_{m}\right\}^{+}(\omega)a_{i,j,k} + \left\{\delta\rho_{m}\right\}^{-}(\omega)b_{i,j,k} + \left\{\delta v_{z,m}\right\}^{-}(\omega)d_{i,j,k}\right), \quad (79)$$

with the coupling coefficients $a_{i,j,k}$, $b_{i,j,k}$, $c_{i,j,k}$ and $d_{i,j,k}$ specified as:

$$a_{i,j,k} = \frac{\mathrm{I}\omega \mathrm{V}_{m}}{2} + A_{m}\left\{v_{z,m}\right\}_{0}^{+}, \quad (80)$$

$$b_{i,j,k} = \frac{\mathrm{I}\omega \mathrm{V}_{m}}{2} - A_{m}\left\{v_{z,m}\right\}_{0}^{-}, \quad (81)$$

$$c_{i,j,k} = A_{m}\left\{\rho_{m}\right\}_{0}^{+}, \quad (82)$$

$$d_{i,j,k} = -A_{m}\left\{\rho_{m}\right\}_{0}^{-}, \quad (83)$$

$$\left\{\delta\rho_{m}\right\}^{+}(\omega) = -\frac{1}{e_{i,j,k} + g_{i,j,k}\beta^{+} - k_{i,j,k}\dfrac{a_{i,j,k}}{c_{i,j,k}} + \dfrac{H_{eff}V_{m}}{2}\dfrac{\mathrm{I}\omega\tau_{f}}{1+\mathrm{I}\omega\tau_{f}}\gamma^{+}}\left[\left\{\delta\rho_{m}\right\}^{-}(\omega)\times\left(f_{i,j,k} + \right.\right.$$

$$\left. h_{i,j,k}\beta^{-} - k_{i,j,k}\frac{b_{i,j,k}}{c_{i,j,k}}\frac{H_{eff}V_{m}}{2}\frac{\mathrm{I}\omega\tau_{f}}{1+\mathrm{I}\omega\tau_{f}}\gamma^{-}\right) + \left\{\delta P_{m}\right\}^{+}(\omega)\left(g_{i,j,k}\alpha^{+} + \frac{H_{eff}V_{m}}{2}\frac{\mathrm{I}\omega\tau_{f}}{1+\mathrm{I}\omega\tau_{f}}\theta^{+}\right) +$$

$$\left\{\delta P_{m}\right\}^{-}(\omega)\left(h_{i,j,k}\alpha^{-} + \frac{H_{eff}V_{m}}{2}\frac{\mathrm{I}\omega\tau_{f}}{1+\mathrm{I}\omega\tau_{f}}\theta^{-}\right) + \left\{\delta v_{z,m}\right\}^{-}(\omega)\left(l_{i,j,k} - k_{i,j,k}\frac{d_{i,j,k}}{c_{i,j,k}}\right) -$$

$$\left.\frac{V_{m}\left\langle\delta q'''\right\rangle(i,j,k,\omega)}{1+\mathrm{I}\omega\tau_{f}}\right], \quad (84)$$

with the coupling coefficients $e_{i,j,k}$, $f_{i,j,k}$, $g_{i,j,k}$, $h_{i,j,k}$, $k_{i,j,k}$ and $q_{i,j,k}$ defined as:

$$e_{i,j,k} = \frac{\mathrm{I}\omega \mathrm{V}_{m}}{2}\left\langle h_{m}\right\rangle_{0}(i,j,k) + A_{m}\left\{v_{z,m}\right\}_{0}^{+}\left\{h_{m}\right\}_{0}^{+}, \quad (85)$$

$$f_{i,j,k} = \frac{\mathrm{I}\omega \mathrm{V}_m}{2}\left\langle h_m \right\rangle_0 (i,j,k) - A_m \left\{ v_{z,m} \right\}_0^- \left\{ h_m \right\}_0^- , \tag{86}$$

$$g_{i,j,k} = \frac{\mathrm{I}\omega \mathrm{V}_m}{2}\left\langle \rho_m \right\rangle_0 (i,j,k) + A_m \left\{ \rho_m \right\}_0^+ \left\{ v_{z,m} \right\}_0^+ , \tag{87}$$

$$h_{i,j,k} = \frac{\mathrm{I}\omega \mathrm{V}_m}{2}\left\langle \rho_m \right\rangle_0 (i,j,k) - A_m \left\{ \rho_m \right\}_0^- \left\{ v_{z,m} \right\}_0^- , \tag{88}$$

$$k_{i,j,k} = A_m \left\{ \rho_m \right\}_0^+ \left\{ h_m \right\}_0^+ , \tag{89}$$

$$q_{i,j,k} = -A_m \left\{ \rho_m \right\}_0^- \left\{ h_m \right\}_0^- , \tag{90}$$

$$\left\{ \delta P_m \right\}^- (\omega) = \frac{1}{r_{i,j,k}}\Big[\left\{ \delta \rho_m \right\}^+ (\omega) m_{i,j,k} + \left\{ \delta \rho_m \right\}^- (\omega) n_{i,j,k} + \left\{ \delta v_{z,m} \right\}^+ (\omega) o_{i,j,k} + \left\{ \delta v_{z,m} \right\}^- (\omega) p_{i,j,k} + \left\{ \delta P_m \right\}^+ (\omega) q_{i,j,k} \Big), \tag{91}$$

with the coupling coefficients $m_{i,j,k}$, $n_{i,j,k}$, $o_{i,j,k}$, $p_{i,j,k}$, $q_{i,j,k}$ and $r_{i,j,k}$ defined as:

$$m_{i,j,k} = \frac{\mathrm{I}\omega \mathrm{V}_m}{2}\left\langle v_{z,m} \right\rangle_0 (i,j,k) + A_m \left[\left\{ v_{z,m} \right\}_0^+ \right]^2 + \frac{F_M V_m}{2D_e \rho_l}\left\langle G_m \right\rangle_0 (i,j,k) \left\langle v_{z,m} \right\rangle_0 + \frac{g V_m}{2}, \tag{92}$$

$$n_{i,j,k} = \frac{\mathrm{I}\omega \mathrm{V}_m}{2}\left\langle v_{z,m} \right\rangle_0 (i,j,k) + A_m \left[\left\{ v_{z,m} \right\}_0^- \right]^2 + \frac{F_M V_m}{2D_e \rho_l}\left\langle G_m \right\rangle_0 \left\langle v_{z,m} \right\rangle_0 (i,j,k) + \frac{g V_m}{2}, \tag{93}$$

$$o_{i,j,k} = \frac{\mathrm{I}\omega \mathrm{V}_m}{2}\left\langle \rho_m \right\rangle_0 (i,j,k) + 2A_m \left\{ G_m \right\}_0^+ (i,j,k) + \frac{F_M V_m}{2D_e \rho_l}\left\langle G_m \right\rangle_0 \left\langle \rho_m \right\rangle_0 (i,j,k), \tag{94}$$

$$p_{i,j,k} = \frac{\mathrm{I}\omega \mathrm{V}_m}{2}\left\langle \rho_m \right\rangle_0 (i,j,k) - 2A_m \left\{ G_m \right\}_0^- (i,j,k) + \frac{F_M V_m}{2D_e \rho_l}\left\langle G_m \right\rangle_0 \left\langle \rho_m \right\rangle_0 (i,j,k), \tag{95}$$

$$q_{i,j,k} = A_m , \tag{96}$$

$$r_{i,j,k} = -A_m . \tag{97}$$

Similar to the static calculations, it was decided to express the corresponding noise equations in terms of node interface quantities rather than node-averaged quantities. The latter fact refers to only axial distribution of the noise, whereas the cross-sectional distributions are still taken for the node-averaged properties. As a result, the above equations provide the coupling between the fluctuations estimated at the interfaces of two pairs of consecutive nodes. If one of these two fluctuations is given, another one can be easily estimated from Eqs. (79), (84) and (91). Thus, providing an initial perturbation at the core inlet (or outlet) for any quantity of interest, the corresponding noise in all other nodes and quantities can be consecutively calculated. However, a detailed analyses of Eqs. (79), (84) and (91) shows that these equations cannot be solved independently from each other due to a nonlinear coupling between the different equations caused by the inclusion of pressure noise calculations.

Therefore, the corresponding solution can be estimated only in an iterative manner. The same problem will then arise when one tries to obtain the full solution for a entire coupled BWR system where the solution is first searched separately for thermo-hydraulic and neutronic models and then both models exchange their outputs until convergence is achieved.

To demonstrate the main principles of the iterative schemes as well as those of the newly-developed model, two block diagrams are presented in *Fig. 4* and *Fig. 5*. In the first figure, the iterative scheme for coupled noise calculations (outer iterations) is illustrated.

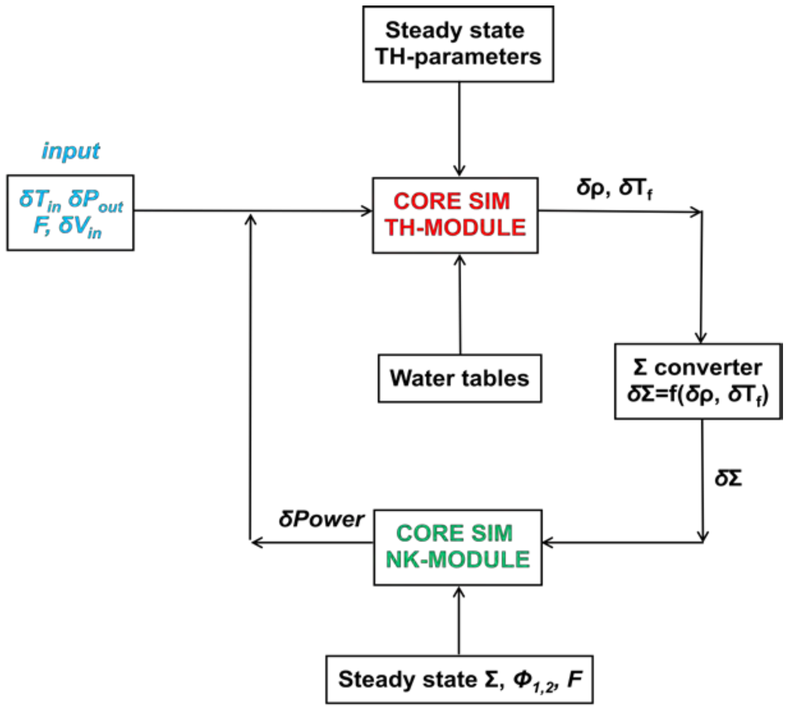

Fig. 4 Coupled dynamic (noise) calculations

As *Fig. 4* shows, this scheme consists of two main modules. The first module, called CORE SIM TH-module contains the set of corresponding thermo-hydraulic equations (79), (84), (91) and is used to calculate the noise in the thermo-hydraulic quantities. As an input, it requires steady–state thermo-hydraulic parameters, water tables and neutron or power noise, and as an output, the noise in the density and fuel temperature is provided. The second block, named as CORE SIM NK-module is based on Eq. (29) and calculates the noise in neutron density. As an input, it needs the steady-state two-group cross sections, neutron fluxes and the neutron noise source, i.e. some perturbation in the cross-sections and as an output it gives fluctuations in the reactor power. There are also two additional small modules called $\sum$-CONVERTER and INPUT included into the first iterative scheme. $\sum$-CONVERTER block incorporates Eq. (76) and converts thermo-hydraulic perturbations into cross-section perturbations. The INPUT block serves as a storage which accepts initial TH-perturbation(s). In the present model, three types of thermo-hydraulic perturbations can be taken into consideration, i.e. a perturbation in inlet velocity (flow), inlet moderator temperature and outlet pressure. In practice, only these quantities can be measured since today's commercial reactors are usually only equipped with inlet temperature sensors, inlet flow meters and outlet pressure sensors. Thus, this latter fact justifies such a specific selection of the quantities being perturbed and makes the choice of any other TH parameters inappropriate (since they cannot be really measured and therefore are not known). In addition, since only the core is actually modelled in this work, these quantities also correspond to the necessary boundary conditions to solve the problem. Then, assuming that the perturbation in the inlet velocity is given, the calculation procedure of the respective noise can be summarized as following:

- calculation of the fluctuations in the density, velocity, enthalpy, moderator temperature, pressure and fuel temperature using CORE SIM TH-module with zero power noise;
- conversion of the density and fuel temperature noise into cross-section fluctuations using $\sum$-CONVERTER;
- calculation of the neutron noise for a given neutron noise source using CORE SIM NK-module;
- the obtained neutron noise source is thereafter used as a power noise source for the next cycle of thermo-hydraulic calculations;
- all previous four steps are repeated until convergence is reached.

The convergence criteria for the outer iterations was imposed on the pressure noise and by default was set to 10^{-9}, i.e. the relative change in the pressure noise between two consecutive iterations should be less than this value.

In *Fig. 5*, the iterative scheme used for the internal thermo-hydraulic noise calculations (inner iterations), is shown. This loop is meant to solve the thermo-hydraulic problem, assuming that the neutron noise (i.e. noise in power) is given.

As can be seen from *Fig. 5*, this scheme contains two separate thermo-hydraulic modules. The first one, designated as TH-module-1 is based on Eqs. (79) ,(84) and calculates the noise in velocity, density, enthalpy and moderator temperature for a fixed (or given) pressure noise (i.e. independently of the pressure noise). As an input for this module, the original TH perturbation, neutron noise, pressure noise and water tables are necessary. The second module, called TH-module-2, is built on the basis of Eq. (91) and estimates the pressure noise for a fixed noise in the other TH- parameters. As input, one needs to provide water tables and the noise in the other TH quantities.

Similarly to the previous case, we again assume that the initial perturbation in inlet velocity is given. Then, the corresponding calculation procedure for the noise can be generalized as:

- calculation of the noise in velocity, density, enthalpy and moderator temperature for a given initial perturbation in the pressure using TH-module-1; here it should be pointed out that in the case of zero perturbation in the outlet pressure, the pressure noise is set to zero for the entire core at the first iteration; if the outlet pressure perturbation is not zero but rather is given as an input, the pressure noise is set to this given (chosen) value at the first iteration, i.e. one follows the same technique as was used in the static pressure calculations;

- calculation of the pressure noise with TH-module-2 for a given velocity/density/enthalpy and moderator temperature noise obtained as a result of the TH-module-1 calculations; here it should be pointed out that the pressure noise calculations are performed in a reversed manner compared to the noise

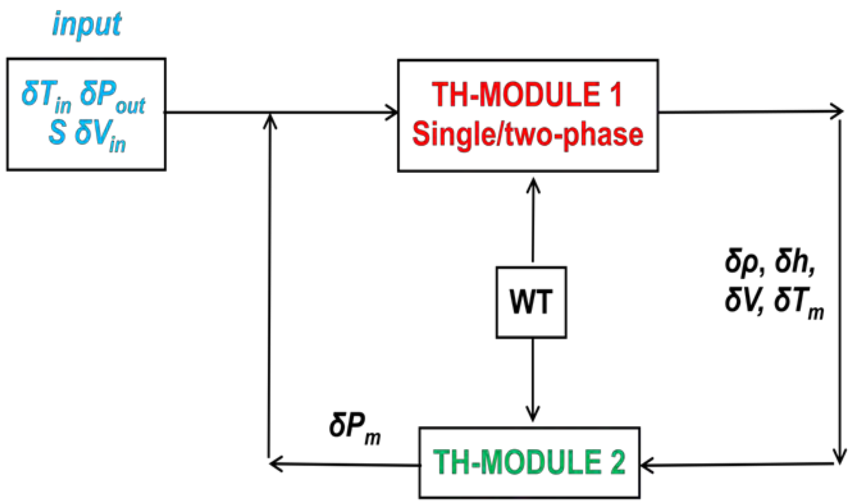

Fig. 5 Internal thermo-hydraulic calculations (pressure calculations, "WT" stands for water tables).

calculations in other quantities; the latter means that the pressure noise calculations are started from the top of the core and proceed to the bottom of the core under the assumption that the pressure noise at the outlet is known as an input (it is set to zero for zero initial pressure fluctuation and is a given input value otherwise); such a reversed calculation procedure can be explained by the fact that, in practice, an outlet pressure is assumed to be known (usually it is fixed to some constant value);

- the pressure noise calculated from TH-module-2 is then used to recalculate the noise in other TH parameters;
- steps 1 to 4 are repeated until the convergence is reached.

The convergence criteria for inner iterations is again imposed on the pressure noise and by default is set to 10^{-21} (in relative terms).

3.3 Results of dynamical calculations

To demonstrate the capabilities of the newly-developed tool, the results of noise simulations performed in the commercial BWR Ringhals-1 at nominal conditions (full power and full core flow) are presented below. As an initial perturbation, a homogeneous perturbation in the inlet velocity was chosen. The calculated amplitudes of the thermal neutron noise, moderator density noise and pressure noise are given in *Fig. 6*-*Fig.* 8. *Fig. 6* shows the amplitude of the radial distribution of the neutron noise at the mid elevation of the core (left figure) and the respective amplitude of the axial variation of the neutron noise in the middle of the core (right figure).

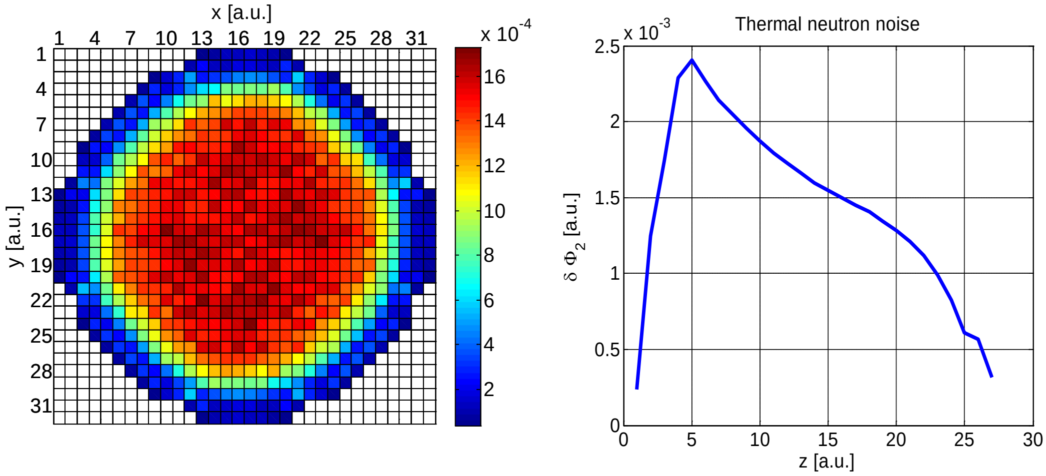

Fig. 6 Radial and axial distribution of thermal neutron noise at $\omega = 1$ rad/s (homogeneous perturbation of inlet velocity $\delta v_{z,m} = 1$ cm/s).

As one can see from *Fig. 6*, the radial distribution of the neutron noise is quite homogeneous over the core active region as can be expected for the case of homogeneous perturbation and it follows the behaviour of the static flux. A similar behaviour can be observed for the axial noise distribution which reconstructs the shape of the static flux with a big peak in the single phase region. The detailed comparison between *Fig. 6* (right figure) and *Fig. 2* indicates that the peak observed in the neutron noise is more pronounced than the one found in the static flux. This apparent inconsistency between two axial distributions can be explained by the fact that the selected frequency of the noise ($\omega = 1$rad/s) is situated in the plateau region of the neutronic transfer function where both space–dependent and point kinetic components of the neutron noise are comparable and thus, both contribute to the total noise.

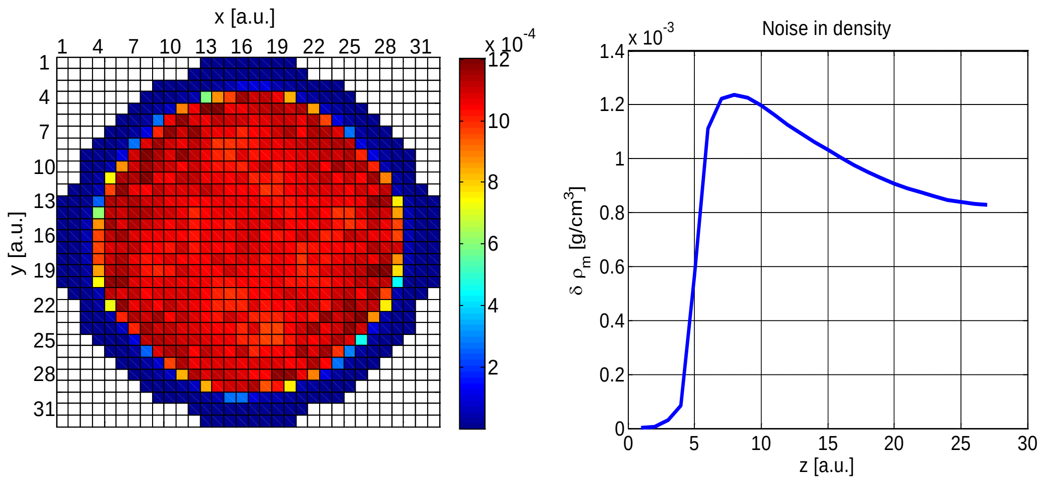

Fig. 7 Radial and axial distribution of the noise in density at $\omega = 1$ *rad/s (homogeneous perturbation of inlet velocity* $\delta v_{z,m} = 1$ *cm/s).*

The corresponding amplitudes of the radial and axial distributions of the noise in coolant density are demonstrated in *Fig. 7*. Similarly to the radial distribution of the neutron noise, the radial distribution of the noise in the coolant density is quite homogeneous, except for the reflector region where the noise level is significantly decreased due to the presence of only one phase. On the other hand, the amplitude of the density noise in axial direction is fully inhomogeneous since both liquid and vapour phases are included. Thus, the amplitude of the density noise first increases in the single phase region and then it starts to decrease in the two-phase region. Comparing *Fig. 7* with *Fig. 3*, one can notice that the axial density noise distribution significantly differs from the static density distribution.

Such a behaviour of the density noise is most likely due to the strong effect of the neutron noise on the fluid moving upwards. In addition, the rather large increase of the density noise in the lower part of the core corresponds to the fluid going from one-phase conditions to two-phase conditions. Because of the large difference between the density of the liquid phase and the one of the vapour phase, any fluctuations at the boiling boundary will result in large density fluctuations.

Finally, the radial and axial distribution of the amplitude of the noise in pressure is discussed (see *Fig. 8*). Similarly to the two previous radial distributions, the radial pressure distribution seems to be quite homogenous (again except for the reflector region) whereas the corresponding axial distribution monotonically decreases, especially in two phase region. Such behaviour is probably caused by the imposed boundary conditions for the pressure noise at the core outlet where the pressure was set to zero. Moreover, the pressure noise contains the contributions due to different pressure components (friction, gravity, acceleration, etc.) which have different phases and different amplitudes in various parts of the core. Such a mixture between different components can also lead to the behaviour of pressure noise noticed above.

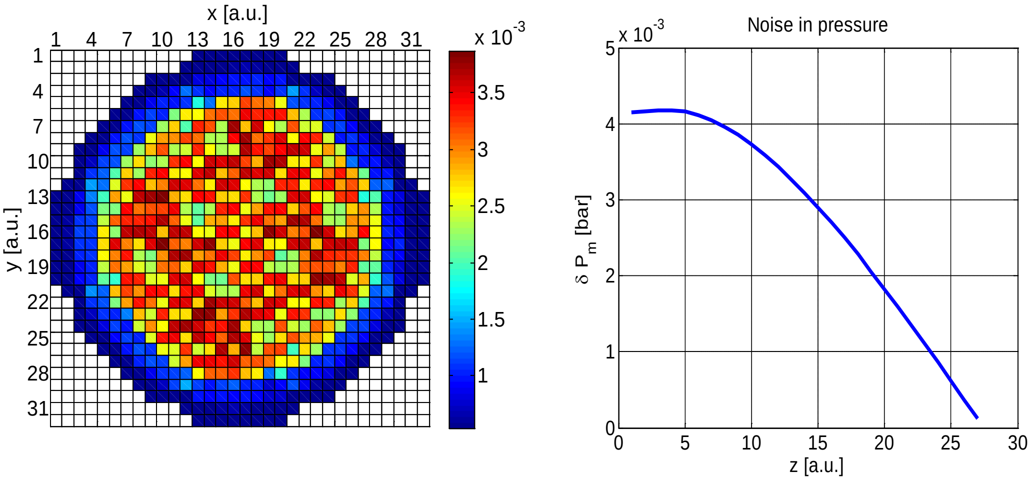

Fig. 8 Radial and axial distribution of the noise in pressure at $\omega = 1$ *rad/s (homogeneous perturbation of inlet velocity* $\delta v_{z,m} = 1$ *cm/s).*

4 Conclusions

An earlier-developed numerical tool called CORE SIM was complemented with a two-phase thermo-hydraulic module in order to be able to calculate fluctuations induced by different perturbations in commercial BWRs. The developed tool is fully MatLab based and requires a set of input data from a commercial static core simulator. This kind of tool is unique and it can treat any heterogeneous system. The driving perturbation can be specified both as a perturbation in thermo-hydraulic parameters or directly as a perturbation in macroscopic cross-sections. The choice of the perturbed thermo-hydraulic quantities is limited to inlet velocity, inlet moderator temperature and core outlet pressure. The effect of each of these perturbations can be studied separately or in combination with several types of perturbations. As output, the 3-dimensional spatial distribution of the noise in coolant density, pressure, enthalpy, inlet velocity, fuel temperature and neutron flux is obtained. In order to validate the simulated results, a benchmark against either real measurements or other codes would be needed. The latter one is planned to be undertaken in the continuation.

The extended CORE SIM core simulator, now being able to treat for PWR and BWR systems, is a useful tool, especially for studying different phenomena taking place in commercial power plants such as, for example, the effect of density wave oscillations and related local instabilities in BWRs. Another application of this tool is that it could be used to indentify the origin of the increasing low-frequency noise level, recently observed in Swedish and German PWRs. Such a work is planned to be performed in the future. As a continuation of the project, it is also planned to develop a unified user-friendly tool which can handle both types of light water reactors, i.e. PWRs and BWRs.

Acknowledgement

This project was supported by the Swedish Radiation Safety Authority, contract No. SSM 2012-3299. Contact person was Assoc. Prof. Ninos Garis.

References

Chisholm D., Pressure gradients due to friction during the flow of evaporating two-phase mixtures in smooth tubes and channels. *Int. J. of Heat Mass and Transfer* **16**, 347-358, 1973.

Demazière C., Development of a 2-D 2-group neutron noise simulator. *Ann. Nucl. Energy* **19**, 647 – 680, 2004

Demazière C. and Pázsit I., Power Reactor Noise, Lecture notes, Chalmers University of Technology, Göteborg, 2008.

Demazière C. and Pázsit I., Numerical tools applied to power reactor noise analysis. *Prog. Nucl. Energy* **51**, 67 – 81, 2009

Demazière C., CORE SIM: A multi-purpose neutronic tool for research and education, *Ann. Nucl. Energy* **38**, 2698-2718, 2011

Forslund P. And Muller E. Parametrization of two-group nodal cross-section data for POLCA BWR transient applications, *IM&C* Saratoga Springs New York, 2009.

Hernández-Solís A., Demazière C. and Ekberg C., Bayesian uncertainty analysis of BWR core parameters based on flux measurements, *ANS Winter Meeting Transactions* **105**, 2011.

Larsson V. and Demazière C., A coupled neutronics/thermal-hydraulics tool for calculating fluctuations in Pressurized Water Reactors, *Ann. Nucl. Energy* 43, 68-76, 2012.

Lindahl S-Ö., *POLCA7-BWR Core Simulator*, Westinghouse Atom AB Report BR 94-700, Rev 2, 2007.

Rust J. H., Nuclear Power Plant Engineering, Haralson Publishing Company, Atlanta, USA, 1979.

Shah R.K., Sekulic D.P., Fundamentals of Heat Exchanger Design, Appendix C. John Wiley & Sons, Inc. 2003.

2014:09

The Swedish Radiation Safety Authority has a comprehensive responsibility to ensure that society is safe from the effects of radiation. The Authority works to achieve radiation safety in a number of areas: nuclear power, medical care as well as commercial products and services. The Authority also works to achieve protection from natural radiation and to increase the level of radiation safety internationally.

The Swedish Radiation Safety Authority works proactively and preventively to protect people and the environment from the harmful effects of radiation, now and in the future. The Authority issues regulations and supervises compliance, while also supporting research, providing training and information, and issuing advice. Often, activities involving radiation require licences issued by the Authority. The Swedish Radiation Safety Authority maintains emergency preparedness around the clock with the aim of limiting the aftermath of radiation accidents and the unintentional spreading of radioactive substances. The Authority participates in international co-operation in order to promote radiation safety and finances projects aiming to raise the level of radiation safety in certain Eastern European countries.

The Authority reports to the Ministry of the Environment and has around 270 employees with competencies in the fields of engineering, natural and behavioural sciences, law, economics and communications. We have received quality, environmental and working environment certification.

Strålsäkerhetsmyndigheten
Swedish Radiation Safety Authority

SE-171 16 Stockholm
Solna strandväg 96

Tel: +46 8 799 40 00
Fax: +46 8 799 40 10

E-mail: registrator@ssm.se
Web: stralsakerhetsmyndigheten.se